Journal of Solid State Chemistry 183 (2010) 1691–1696

Contents lists available at ScienceDirect

Journal of Solid State Chemistry

journal homepage: www.elsevier.com/locate/jssc

Neutron scattering study of water confined in periodic mesoporous organosilicas

Esthy Levy [a], Lok Kay Chan [b], Dehong Yu [c], Michael Marek Koza [d], Yitzhak Mastai [a,*], R.C. Ford [b], Jichen Li [e]

[a] Department of Chemistry, Institute of Nanotechnology, Bar-Ilan University, Israel
[b] Faculty of Life Sciences, University of Manchester, United Kingdom
[c] Bragg Institute, Australian Nuclear Science and Technology Organisation, PMB 1, Menai NSW 2234, Australia
[d] Institute Laue Langevin, 6 rue Jules Horowitz, BP156, F-38042 Grenoble, France
[e] Department of Physics and Astronomy, University of Manchester, Manchester, UK

ARTICLE INFO

Article history:
Received 27 December 2009
Received in revised form
10 May 2010
Accepted 17 May 2010
Available online 20 May 2010

Keywords:
Water
Ice
Mesoporous organosilica
Inelastic neutron scattering
Porous solids

ABSTRACT

A series of quasi-elastic neutron scattering measurements were performed using IN6 at the Institute Laue Langevin for a mesoporous organosilica material with phenyl functions, called phenyltriethoxysilane (PTES). The aim of the experiment was to study the diffusion dynamics of nano-scale water clusters inside the hydrophobic pores as a function of temperature and hydration. By fitting the Debye–Waller factor, the data show clearly the different behavior between water, both inside and outside the hydrophobic pores, which resembles bulk water. The mean thermal displacement $\langle u^2 \rangle$ of the external water increases with T almost linearly up to 353 K, while the internal water quickly reaches the maximum at $T \sim 323$ K, indicating the confinement by an averaged pore diameter of the porous organosilica.

1. Introduction

The properties of materials geometrically confined on a nanometer spatial scale have attracted considerable attention over the two last decades [1–5]. There is increasing interest in the application of "nanoscale materials"; however, a good understanding of their microscopic properties is still lacking, especially those relating to the dynamics of confined systems. Experimentally, a strong change of the dynamic properties of spatially restricted materials with respect to their bulk properties is now well established. Nevertheless, the influence of the confining materials, the geometry of pores and especially the role of the interaction with interfaces compared to a possibly restricted intrinsic correlation length is not yet fully understood. Dynamics in confinement appears for many phenomena, starting from the clear case, where atoms, molecules, liquids or solids are enclosed in 3-dimensional cavities of porous systems, over cases where atoms or molecules are restricted to move in 2D, like in the galleries of clays, in very thin films or at surfaces and finally to cases, where confinement may have some but not the major influence on the dynamics, like for water confined in biological systems or copolymers, where soft polymer phases are surrounded by glassy polymer phases.

Water, when it is confined or in contact with substrates, plays an important role in many natural processes. Water can be confined in rocks, in biological cells, at contact with surfaces of proteins, and in membranes. The interplay between the thermodynamic and the dynamic properties of water [6,7] and the substrate is essential in many natural processes like, for instance, the enzymatic activity of globular proteins or the functionality of biological membranes [8,9]. In spite of the large variety of geometrical and physical properties of the substrates, some general trends are observed in confined water, such as in pores of porous silica [10–17].

The structure of porous silica consists of an enormous network of interconnected pores. When it is hydrated, water fills these pores and is confined in the microscopic geometric space. Therefore, porous silica offers an ideal environment for research on water behavior in a confined space. In addition, mesoporous silica is a material with a sufficiently homogeneous structure, and the geometric sizes of its pores structure are very well defined, usually a few nanometers.

The structural and dynamic properties of bulk water are already widely well known. The behavior of bulk water at different ranges of temperature and pressure has been intensively investigated in the last few years, using different techniques such

* Corresponding author.
E-mail address: mastai@mail.biu.ac.il (Y. Mastai).

0022-4596/$ - see front matter © 2010 Elsevier Inc. All rights reserved.
doi:10.1016/j.jssc.2010.05.017

as the X-ray diffraction [18,19], neutron scattering for ice (NS) [20,21], nuclear magnetic resonance (NMR), etc.

It is well known that water molecules form a great variety of hydrogen bond networks, i.e., pure water has many polymorphs whose structures are varied by the interaction with surfaces. The structure and dynamics of water are modified by the presence of surfaces via a modification of hydrogen bonding and by alteration of molecular motion. These effects strongly depend on the distance of water molecules from the surface. Therefore, a detailed description of these properties must take into account the polarity of the surface and its affinity to form bonds with water molecules, and the hydration level—in other words, the number of water layers.

In order to discriminate between these effects, reliable model systems exhibiting hydrophilic or hydrophobic interactions with water are required. In this paper, we present new results experimenting with water inside mesoporous hybrid materials functionalized with organic groups (facing into the pore channels). We will show that confined water (also known as "interfacial" water [10]) is strongly influenced by the polarity of the organic groups bound to the wall surfaces. In this paper, we focused on hydrophobic mesoporous silica materials.

Recently, the structural and dynamic properties of water in a confined space, such as in silica gel and Vycor glass, have also been investigated [15,22–29]. In 1999, a study using the X-ray technique was performed by Morineau et al. [30] on the freezing and melting behavior of water in MCM-41, a type of porous media with a structure of cylindrical pores hexagonally embedded in amorphous silica. Eight samples with different pore sizes were prepared. They found that at a temperature of 232 K, water confined in a space the size of 42 Å freezes very quickly into cubic ice, and behaves quite differently from its bulk form. Recently, research was also carried by Bellissent-Funel et al. [12] using a quasi-elastic neutron scattering (QENS) technique for the freezing properties of water in Vycor glass. The crystallization of cubic ice was observed at a temperature of 255 K. In 2001, a book [31] was published summarizing research on water confined in silica gel at different temperatures, using X-ray techniques.

While inorganic periodic mesoporous silica alone may be suitable for some applications, researchers have recently realized that the properties of mesoporous materials could be modified by including organic groups in the channel spaces. Lately, a new class of mesoporous materials, called periodic mesoporous organosilicas (PMOs), has been reported [32–35]. These materials are unique compared to the first generation periodic mesoporous silica materials, since the channel walls contain both organic and inorganic substances. This marriage of organic chemistry with inorganic materials chemistry offers fascinating new possibilities and applications. The organic functionalisation of periodic mesoporous organosilicas permits changes in the surface properties: hydrophilicity, hydrophobicity, binding to guest molecules, etc., and modification of the pore and the bulk properties of water. The PMOs materials can be synthesized with a wide variety of organic groups (R) [3,36–42]. In this work, we prepared mesoporous organosilica materials with phenyl group on the internal and external pore surfaces: PTES [42] (phenyltriethoxysilane, its chemical structure is shown in Fig. 1).

Indeed, the properties of the mesoporous materials could be modified by including organic groups in the channel spaces or into the silica walls [43–45]. Organic modifications of these solids allow accurate control of the surface properties and the pore size distribution. Even modification of the bulk properties of the water confined in these solids is possible by incorporating organic groups in the porous solid. In this paper, we present, in addition to the synthesis of the mesoporous materials, a description of the dynamics of confined water inside these PMOs materials with different hydrations (dry, 30% and 60%, hydrated, respectively) using Quasi-Elastic Neutron Scattering (QENS) instrument, namely IN6, at low temperatures.

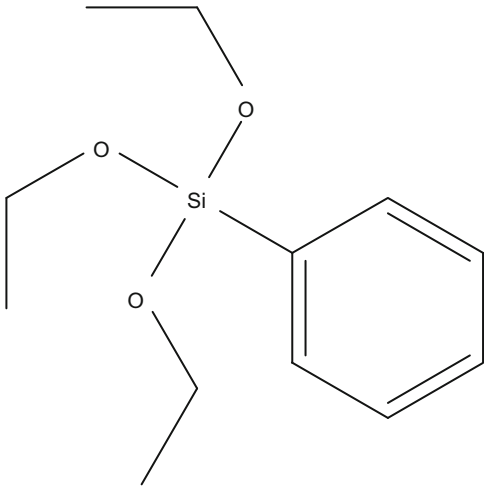

phenyltriethoxysilane

PTES

Fig. 1. Structure of phenyltriethoxysilane (PTES) periodic mesoporous organosilicas.

2. Experimental part

2.1. Synthesis of PTES

Inorganic–organic mesoporous silica was synthesized at room temperature from mixtures containing a constant molar ratio of a functionalized organotrialkoxysilane (PTES) with tetraethoxysilane (TEOS) in the presence of the surfactant, C_{16}TAB. For the synthesis of the periodic mesoporous organosilicas, a solution composed of a molar ratio of Si:C_{16}TAB:H_2O:NH_4OH of 1.0:0.12:130.1:0.5 was prepared. Typically, a solution was made of water (2.34 ml 0.13 mol) ammonium hydroxide (0.02 g, 0.5 mmol) and C_{16}TAB (0.044 g, 0.12 mmol). The surfactant was dissolved by warming the solution to 313 K, after which a mixture containing a constant molar ratio of phenyltriethoxysilane (0.048 g, 0.2 mmol) with tetraethoxysilane (0.17 g, 0.8 mmol) was added drop wise to this solution with rapid stirring. PTES and TEOS were mixed before addition to the surfactant solution. Once the solution had homogenized, the stirring was slowed down for an additional 10 min. After aging at 353 K for four days, the product was isolated by filtration as a white powder.

2.2. Surfactant-extraction

The surfactant template was removed from the organosilica materials through a solvent extraction process. A 2 g sample of the product was refluxed in 3 ml of (37 wt%) HCl/200 ml of methanol for 1 day, collected by suction filtration, washed with water, and dried in air at room temperature.

2.3. Characterization

Small-angle X-ray scattering (SAXS) patterns in a range of 2θ angles from 2° to 8° were recorded on a Brucker AXS D8 Advance Diffractometer (using CuKα λ=1.5418 Å radiation) operating at

40 kV/40 mA, with a graphite-reflected beam monochromator and variable divergence slits. Sorption isotherms of nitrogen at 77 K were measured by gas volumetry using a Quantachrome Autosorb-1 system. High resolution transmission electron microscopy (HR-TEM) images were acquired on a JEOL 840 instrument with an acceleration voltage of 200 kV.

2.4. Quasi-elastic neutron scattering (QENS)

The QENS experiments were performed on the IN6 at the Institut Laue-Langvin (ILL) in Grenoble. The cold neutron time-focusing time-of-flight (TOF) spectrometer allows quasi-elastic and inelastic scattering for incident wavelengths in the range 4–6 Å. Over 340 detectors covering different angles allow a large range of momentum transfer Q values to be collected, for which subtle effects can be identified accurately. This was a key factor in the design of the experiment due to the measurement of the Debye–Waller effect within the samples. The intensity of the spectrum gained is expressed as

$$I(Q, \omega) = e^{-(Q^2 < \mu^2(T) >)} S(Q, \omega). \quad (1)$$

The Debye–Waller factor, $W(=Q^2\langle\mu^2\rangle)$, is used to describe the propagation of the nucleus from its equilibrium, caused by thermal motion; μ, can be assumed to be primarily dependent on temperature, T, and $\langle\mu^2\rangle$ represents the mean squared vibrational displacement. For a given Q, $W(Q)$ gives the fraction of elastic scattering. By varying the temperature of the sample, the sensitive QENS technique allows for the vibrations within the quasi-elastic region to be derived for values of Q, the momentum transfer between the neutron and nucleus. Over 300 spectra were used in the analysis at each given temperature, and μ was discretely derived at a given Q value.

The IN6 instrument allowed an extensive range in the sample's temperature to be achieved. Utilizing this, spectra of the sample were obtained from 100 K through to 353 K. At temperatures below 270 K, readings were taken at increments of 10 K, whilst at 273 K and above, a spectrum was recorded for every 2 K increment. Time was allowed between readings for the temperature adjustment to stabilize.

Porous PTES silica was prepared on site by vacuuming 1 g for the dry sample overnight. For the dry sample, 1 g of porous PTES silica was placed in a 0.3 mm thick aluminum cell. These measurements were chosen to ensure a smooth consistent area between the plates of the sample that is exposed to the neutron beam, while taking into consideration the limitations posed by multi-scattering effects and to optimize the one-phonon scattering of the neutrons. Even the 1 g of dry organosilica caused significant neutron scattering to be detected. With the addition of H_2O, this would increase the number of hydrogen atoms significantly, and since neutrons are particularly susceptible to hydrogen atoms, it is important to ensure that multi-phonon scattering does not pose a problem with the data. For the wet samples, the amount of organosilica was reduced to 0.5 g. Hydrations of organosilica with H_2O were prepared at 30% and 60%. The wet samples (0.5 g of porous PTES silica with the appropriate amounts of H_2O) were placed between two flat circular aluminum plates with a sample thickness of 0.5 mm. Readings were taken from high to low temperatures to ensure a dry environment. The exposure time to the neutron beam also had to be considered; the smaller the sample inside the cell, the longer is the duration of beam time needed. The dry organosilica was allowed 20 min per run, 35 min per run for the 60% hydrated sample and 45 min per run for the 30% hydrated sample. Every care was taken to ensure that once the hydrated samples were prepared in the cell, dehydration was kept to a minimum. The aluminum plates were twisted tightly together with a rubber band. Samples were only prepared just prior to insertion into the instrument, and readings were taken from high to low temperatures.

3. Results and discussion

3.1. Characterization and structure of the PTES sample

The small-angle X-ray scattering (SAXS) patterns in a range of 2θ angles from 2° to 8° of the PTES sample are shown in Fig. 2a. The PTES material exhibits three well-resolved peaks and the peak pattern conforms to a two-dimensional hexagonal lattice (space group *p6*mm). A high resolution transmission electron microscopy (HR-TEM) image of the PTES sample is shown in Fig. 2b. It can be seen that a highly porous material with the so-called "wormhole structure" with disordered pores is produced with an average pore size of around 40 Å. Nitrogen adsorption for the PTES material is shown in Fig. 2(c) and (d). The sorption isotherm exhibits a type IV isotherm characteristic of mesoporous materials. A nitrogen adsorption experiment performed on a surface-extracted PTES sample yielded a BET calculated surface area of 295 $m^2\,g^{-1}$, and narrow pore size distribution of 35 Å (see Fig. 2(d)) by applying the BJH (Barrett–Joyner–Halenda) method. IR spectrum of PTES sample after reflex (surfactant-extraction) at 80 °C is shown in Fig. 2e. The FT-IR spectra of PTES exhibit several typical absorption bands of the incorporated organic group such as: aromatic ring C–C stretches at 1591 cm^{-1}; aromatic C–H bends at 740 and 700 cm^{-1} and the most typical and important band of aromatic C–Si stretch at 1430 cm^{-1}. Those FTIR results prove that our PTES sample is a true organosilica with the incorporation of the organic–inorganic precursors into the porous.

3.2. QENS measurements

The QENS technique is used for studying stochastic motions, and has been successfully used to explain the molecular motions and physical properties in a variety of systems. QENS is also a unique technique that provides information on the time scale of the motion as well as the geometry of the structure involved. QENS probes the dynamics of matter at very low energies. At low energies, the neutrons are more likely to interact elastically, but even during this interaction, which is conventionally regarded as 'no interaction,' the nucleus is still displaced to some extent. This displacement allows for the interpretation of both the dependence of the Debye–Waller factor as well as information regarding the structure term. It is known that confined water behaves differently to free water and is worth studying in order to give more information on the overall theme of water interaction in biological systems. This is also an important area of research for water interaction within nanostructures. Due to the QENS sensitivity to hydrogen atoms, this technique is particularly favorable for the study of water, and has already been successful for several systems, including DNA [46].

The QENS spectra of organosilica with different hydrations, $S(Q, \omega)$, was modeled in two components, including Gaussian and Lorentzian peak shapes. They are demonstrated as follows: a resolution-limited Gaussian lineshape of width w and integrated area A was used to model the elastic peak representing the organosilica with frozen water. A Lorentzian lineshape of broadening width w and integrated area B was used to model the quasi-elastic broadened component representing the signal from liquid water in organosilica. A constant background was used to model the background signal generated by the experimental equipment.

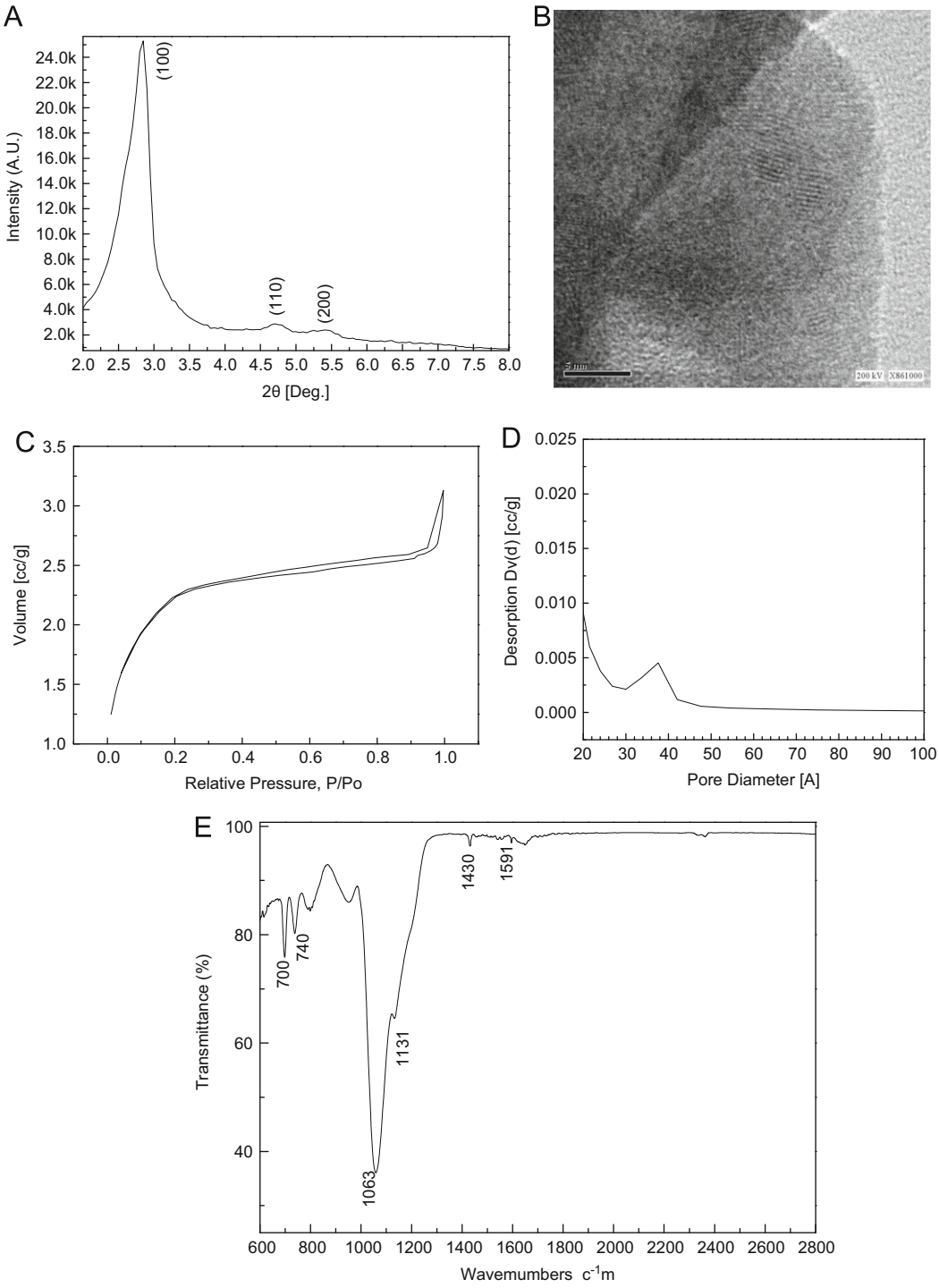

Fig. 2. (a) Small-angle X-ray scattering pattern; (b) high resolution transmission electron micrograph (HR-TEM) showing the periodic arrangement of the pores in a PTES silica sample; (c) nitrogen adsorption isotherm of the PTES sample; (d) pore size distribution using BJH method and (e) IR spectrum of PTES sample after reflex (surfactant-extraction) at 80 °C.

The graphing and data analysis software, Origin, was used to analyze the QENS data. The method is outlined in Eq. (2)

$$S(Q,\omega) = \frac{A}{w\sqrt{\pi/2}} e^{-2((x-x_c)^2/w^2)} + \frac{2B}{\pi} \frac{W}{4(x-x_c)^2 + W^2} + C, \qquad (2)$$

where w is the width of the Gaussian lineshape, W is the Lorentzian broadening width, χ is the energy transfer, χ_c is the centre of the quasi-elastic peak, A, B are the integrated areas of Gaussian and Lorentzian parts, respectively, and C is the background signal. The values of W were determined at temperatures ranging from 15 to around 90 °C for the organosilica with two different hydrations: 30% and 60%, respectively (see figure in supporting information, S1).

In a series of QENS measurements for the sample with 30% water shown in Fig. 3, the effect of temperature on hydrated porous PTES silica is presented. In the QENS measurements, the presence of fast moving particles, such as water molecules, is shown by a broad peak. This is reflected within the experimental data. At higher temperatures each situation shows a broadening of the peak, due to interactions between the nucleus and the

neutrons. At low temperatures, it is more likely for an elastic collision to occur, i.e., for the neutron not to experience any exchange of energy, and hence a more defined peak and lower distribution in the overall energy range are observed. At very low temperatures, the broadening is less prominent due to reduction in thermal motions and multi-phonon combinations as the probability of vibrational activity is lower. It does appear that at temperatures above 200 K, even though the sample is frozen, there is sufficient thermal energy to cause molecular activity.

Plotting of the Debye–Waller factor $W(=\ln[(I(Q)/S(Q))])$ against Q^2 at QENS peak positions for each temperature shows very strange behavior, instead of a straight line predicated by Eq. (1). There are two different $\langle\mu^2\rangle$ gradients present for the high temperature curves, one at very low values of Q and the other at higher values of Q, as seen in Fig. 4 for the sample with 30% at different temperatures. We believe that may be due to two types of water present in this sample; one is associated with the water inside the pores and the other is outside (external), which is much like bulk water.

At very low temperatures, where any molecular motion is very limited, the lines appear straight (i.e., the water inside and outside has the sample gradient). However, as the temperature is increased, the low Q region experiences a higher exponential decrement than at high Q. One could assume two sets of gradients to interpret this effect since "internal" and "external" water is present within the hydrated samples. The Debye–Waller function

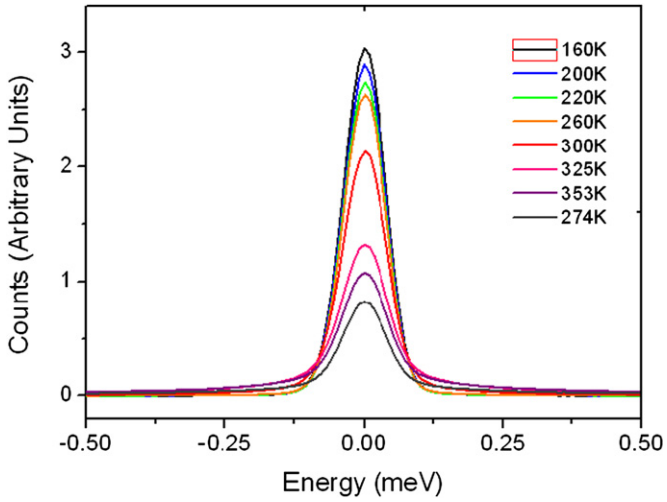

Fig. 3. The plot shows a series of QENS measurements for the porous PTES silica with 30% hydration (wt%) as a function of temperature, from 160 to 352 K.

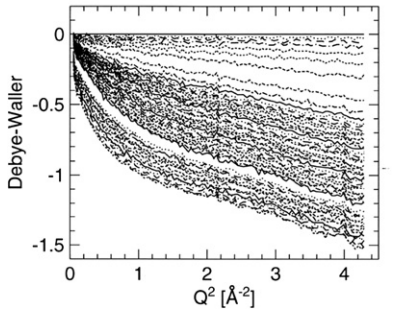

Fig. 4. Debye–Waller *vs.* Q^2 of porous PTES silica hydrated at 30% water (wt%). The different curves are for different temperatures. The top curve is for T at 160 K and the bottom one is for T at 352 K. The measurements are made at 10 K per step between 160 and 270 and 2 K per step between 270 and 352 K.

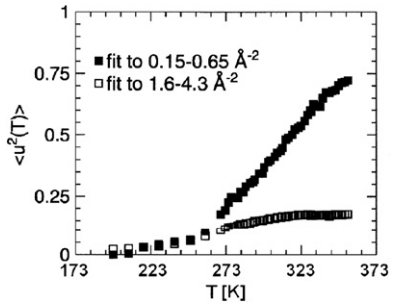

Fig. 5. Plot of $\langle\mu^2\rangle$ *vs.* temperature for the porous PTES silica with 30% hydration (wt%). Open squares are the data representing internal water and solid squares are for the external water.

was fitted appropriately with respect to each of the gradients (Fig. 4). For each cell condition, the different fits produce two very different results for the Debye–Waller factor. There is a clear evidence that two types of water molecules are present, surface bonded molecules to the porous organosilica contribute to local restricted motion at high Q values. Other water molecules undergo diffusion within the regions surrounding the porous organosilica, which is at a low Q region. The amplitude of thermal motion $\langle\mu^2\rangle$ from external bulk-like water.

It is reasonable to assume that water confined within the pores and bonded to the surface of silica would experience restrictions in its movement. This is supported by the hydrated QENS data in Fig. 5. Below 273 K, the graphs for both low and high Q appear similar, and there is even a phase change indicated in the graphs, which would be typical for the solid–liquid transition. However, it is at temperatures above freezing that the data become more intricate. For low Q values at temperatures above 273 K, a steep linear sequence of points indicates a proportional relationship between temperature and the motion of the molecules. For example, a rise in temperature leads to an increment in the displacement of the molecules. One would interpret the steep $\langle\mu^2\rangle$ gradient from low Q to be characteristic of that of bulk water behavior. However, this relationship is very different at high Q, where the data reveal the relationship to be constricted, and where a high increase in temperature would only result in a very subtle change of $\langle\mu^2\rangle$. This would imply that the motion of internal water is heavily restricted, which correlates with the geometry of the mesoporous organosilica itself. Thus, the confined local water molecules and the first few monolayers of the organosilica are those inhibited within the pores.

However, the number of interfacial layers has not been defined in these results. There have been studies to show that rotational dynamics of water molecules within the pores compared to bulk water do not change at room temperature [47]. The results from the Debye–Waller fitting indicate that below freezing there are vibrational similarities between bulk and confined water. One could suggest that above freezing, when the translational motion of the water molecules is susceptible; this is where the confined water molecules find its limitations.

4. Conclusions

The QENS technique was applied to study various dynamical parameters of water in periodic mesoporous organosilica based on PTES at temperature range 353–100 K. It is seen that the water molecules attached to the surface of the PTES mesoporous silica perform very local motion compared to the water outside the pores.

Appendix A. Supplementary material

Supplementary data associated with this article can be found in the online version at doi:10.1016/j.jssc.2010.05.017.

References

[1] C. Alba-Simionesco, B. Coasne, G. Dosseh, G. Dudziak, K.E. Gubbins, R. Radhakrishnan, M. Sliwinska-Bartkowiak, Journal of Physics–Condensed Matter 18 (2006) R15–R68.
[2] C. Faivre, D. Bellet, G. Dolino, European Physical Journal B 7 (1999) 19–36.
[3] C.L. Jackson, G.B. Mckenna, Journal of Chemical Physics 93 (1990) 9002–9011.
[4] R. Mu, V.M. Malhotra, Physical Review B 44 (1991) 4296–4303.
[5] R. Mu, Y. Xue, D.O. Henderson, D.O. Frazier, Physical Review B 53 (1996) 6041–6047.
[6] G. Buntkowsky, H. Breitzke, A. Adamezyk, F. Roelofs, T. Emmler, E. Gedat, B. Grunberg, Y. Xu, H.H. Limbach, J. Shenderovich, A. Vyalikh, G. Findenegg, Physical Chemistry Chemical Physics 9 (2007) 4843–4853.
[7] E. Tombari, G. Salvetti, C. Ferrari, G.P. Johari, Journal of Chemical Physics 122 (2005) 104712.
[8] G.W., Robinson Water in Biology Chemistry and Physics, 1999.
[9] P.G. Debenedetti, in: Metastable Liquids: Concepts and PrinciplesPrinceton University Press, Princeton, 1997.
[10] M.C. Bellissent-Funel, European Physical Journal E 12 (2003) 83–92.
[11] M.C. Bellissent-Funel, K.F. Bradley, S.H. Chen, J. Lal, J. Teixeira, Physica A 201 (1993) 277–285.
[12] M.C. Bellissent-Funel, S.H. Chen, J.M. Zanotti, Physical Review E 51 (1995) 4558–4569.
[13] M.C. Bellissent-Funel, J. Lal, L. Bosio, Journal of Chemical Physics 98 (1993) 4246–4252.
[14] L. Bosio, G.P. Johari, M. Oumezzine, J. Teixeira, Chemical Physics Letters 188 (1992) 113–118.
[15] Y.P. Handa, M. Zakrzewski, C. Fairbridge, Journal of Physical Chemistry 96 (1992) 8594–8599.
[16] D.C. Steytler, J.C. Dore, Molecular Physics 56 (1985) 1001–1015.
[17] D.C. Steytler, J.C. Dore, C.J. Wright, Journal of Physical Chemistry 87 (1983) 2458–2459.
[18] P.A. Egelstaff, Advances in Chemical Physics 53 (1983) 1–60.
[19] A.V. Okhulkov, Y.N. Demianets, Y.E. Gorbaty, Journal of Chemical Physics 100 (1994) 1578–1588.
[20] J.C. Li, C. Burnham, A.I. Kolesnikov, R.S. Eccleston, Physical Review B 59 (1999) 9088–9094.
[21] M.C. Bellissent-Funel, L. Bosio, Journal of Chemical Physics 102 (1995) 3727–3735.
[22] M. Brun, A. Lallemand, J.F. Quinson, C. Eyraud, Thermochimica Acta 21 (1977) 59–88.
[23] J.F. Quinson, M. Brun, Characterization of Porous Solids, In: K.K. Unger, J. Rouquerol, K.S.W. Sing, H. Kral (Eds.), Elsevier, Amsterdam, 1988.
[24] E. Molz, A.P.Y. Wong, M.H.W. Chan, J.R. Beamish, Physical Review B 48 (1993) 5741–5750.
[25] A. Fouzri, R. Dorbez-Sridi, M. Oumezzine, Journal of Chemical Physics 116 (2002) 791–797.
[26] Y. Wang, S.L. Dong, Chinese Physics Letters 19 (2002) 711–713.
[27] E. Levy, A.I. Kolesnikov, J.C. Li, Y. Mastai, Surface Science 603 (2009) 71–77.
[28] A. Fouzri, R. Dorbez-Sridi, S. Nasr, M. Oumezzine, Biomolecular Engineering 19 (2002) 207–210.
[29] A. Fouzri, R. Dorbez-Sridi, M. Oumezzine, A. Missaoui, International Journal of Inorganic Materials 3 (2001) 1315–1317.
[30] D. Morineau, G. Dosseh, C. Alba-Simionesco, P. Llewellyn, Philosophical Magazine B—Physics of Condensed Matter Statistical Mechanics Electronic Optical and Magnetic Properties 79 (1999) 1847–1855.
[31] Kallay, N. Interfacial Dynamics CRC Press Ed., 2000.
[32] O. Dag, C. Yoshina-Ishii, T. Asefa, M.J. MacLachlan, H. Grondey, N. Coombs, G.A. Ozin, Advanced Functional Materials 11 (2001) 213–217.
[33] S. Inagaki, S. Guan, Y. Fukushima, T. Ohsuna, O. Terasaki, Journal of the American Chemical Society 121 (1999) 9611–9614.
[34] B.J. Melde, B.T. Holland, C.F. Blanford, A. Stein, Chemistry of Materials 11 (1999) 3302–3308.
[35] C. Yoshina-Ishii, T. Asefa, N. Coombs, M.J. MacLachlan, G.A. Ozin, Chemical Communications (1999) 2539–2540.
[36] G. Temtsin, T. Asefa, S. Bittner, G.A. Ozin, Journal of Materials Chemistry 11 (2001) 3202–3206.
[37] C. Li, Catalysis Reviews—Science and Engineering 46 (2004) 419–492.
[38] T. Asefa, M. Kruk, N. Coombs, H. Grondey, M.J. MacLachlan, M. Jaroniec, G.A. Ozin, Journal of the American Chemical Society 125 (2003) 11662–11673.
[39] M.H. Lim, C.F. Blanford, A. Stein, Journal of the American Chemical Society 119 (1997) 4090–4091.
[40] M.H. Lim, C.F. Blanford, A. Stein, Chemistry of Materials 10 (1998) 467 – +.
[41] C.E. Fowler, S.L. Burkett, S. Mann, Chemical Communications (1997) 1769–1770.
[42] M. Kuroki, T. Asefa, W. Whitnal, M. Kruk, C. Yoshina-Ishii, M. Jaroniec, G.A. Ozin, Journal of the American Chemical Society 124 (2002) 13886–13895.
[43] R.J.P. Corriu, A. Mehdi, C. Reye, C. Thieuleux, Chemical Communications (2002) 1382–1383.
[44] T. Asefa, C. Yoshina-Ishii, M.J. MacLachlan, G.A. Ozin, Journal of Materials Chemistry 10 (2000) 1751–1755.
[45] A. Stein, B.J. Melde, R.C. Schroden, Advanced Materials 12 (2000) 1403–1419.
[46] R.C. Ford, S.V. Ruffle, A.J. Ramirez-Cuesta, I. Michalarias, I. Beta, A. Miller, J.C. Li, Journal of the American Chemical Society 126 (2004) 4682–4688.
[47] S. Mitra, R. Mukhopadhyay, I. Tsukushi, S. Ikeda, Journal of Physics—Condensed Matter 13 (2001) 8455–8465.